



Published in final edited form as:

J Hepatol. 2015 December ; 63(6): 1397–1404. doi:10.1016/j.jhep.2015.07.020.

Exposure to Fine Airborne Particulate Matters Induces Hepatic Fibrosis in Murine Models

Ze Zheng¹, Xuebao Zhang¹, Jiemei Wang¹, Aditya Dandeka², Hyunbae Kim¹, Yining Qiu¹, Xiaohua Xu⁴, Yuqi Cui³, Aixia Wang^{3,4}, Lung Chi Chen⁵, Sanjay Rajagopalan³, Qinghua Sun^{3,4}, and Kezhong Zhang^{1,2,*}

¹Center for Molecular Medicine and Genetics, Wayne State University School of Medicine, Detroit, MI 48201, USA

²Department of Immunology and Microbiology, Wayne State University School of Medicine, Detroit, MI 48201, USA

³Division of Cardiovascular Medicine, Davis Heart & Lung Research Institute, College of Medicine, Ohio State University, Columbus, OH 43210, USA

⁴Division of Environmental Health Sciences, College of Public Health, Ohio State University, Columbus, OH 43210, USA

⁵Department of Environmental Medicine, New York University, Tuxedo, NY 10987, USA

Abstract

Background—Hepatic fibrosis, featured by accumulation of excessive extracellular matrix in liver tissues, is associated with metabolic disease and cancer. Inhalation exposure to airborne particulate matter in fine ranges (PM_{2.5}) correlates with pulmonary dysfunction, cardiovascular disease, and metabolic syndrome. In this study, we investigated the effect and mechanism of PM_{2.5} exposure on hepatic fibrogenesis.

Methods—Both inhalation exposure of mice and *in vitro* exposure of specialized cells to PM_{2.5} were performed to elucidate the effect of PM_{2.5} exposure on hepatic fibrosis. Histological examinations, gene expression analyses, and genetic animal models were utilized to determine the effect and mechanism by which PM_{2.5} exposure promotes hepatic fibrosis.

Results—Inhalation exposure to concentrated ambient PM_{2.5} induces hepatic fibrosis in mice under the normal chow or high-fat diet. Mice after PM_{2.5} exposure displayed increased expression

*Corresponding Authors: Kezhong Zhang, Ph.D., 540 E. Canfield Avenue, Detroit, MI 48201, Tel: 313-577-2669; FAX: 313-577-5218; k Zhang@med.wayne.edu.

Publisher's Disclaimer: This is a PDF file of an unedited manuscript that has been accepted for publication. As a service to our customers we are providing this early version of the manuscript. The manuscript will undergo copyediting, typesetting, and review of the resulting proof before it is published in its final citable form. Please note that during the production process errors may be discovered which could affect the content, and all legal disclaimers that apply to the journal pertain.

Conflict of interest statement: the authors Z.Z., X.Z., J.W., A.D., H.K., Y.Q., X.X., Y.C., A.W. L.C.C., S.R., Q.S., and K.Z. have nothing to declare.

Authors' contributions: study concept and design: K.Z., Z.Z., Q.S.; acquisition of data, analysis and interpretation of data: Z.Z., K.Z., Q.S., X.Z., J.W., A.D., H.K., Y.Q., A.W.; drafting of the manuscript: K.Z., Z.Z.; critical revision of the manuscript for important intellectual content: K.Z., Z.Z., Q.S.; statistical analysis: Z.Z., X.Z., J.W., A.D., X.X., Q.S.; obtained funding: Z.Z., Q.S.; administrative, technical, or material support: X.X., Y.C., A.W., L.C.C., S.R.; study supervision: K.Z., Q.S.

of collagens in liver tissues. Exposure to PM_{2.5} led to activation of the transforming growth factor β (TGF β)-SMAD3 signaling, suppression of peroxisome proliferator-activated receptor γ (PPAR γ), and expression of collagens in hepatic stellate cells. NADPH oxidase plays a critical role in PM_{2.5}-induced liver fibrogenesis.

Conclusions—Exposure to PM_{2.5} exerts discernible effects on promoting hepatic fibrogenesis. NADPH oxidase mediates the effects of PM_{2.5} exposure on promoting hepatic fibrosis.

Introduction

Recent studies indicated that exposure to fine ambient particulate matter (aerodynamic diameter < 2.5 μm , PM_{2.5}) is a risk factor for pulmonary and cardiovascular diseases as well as metabolic syndrome [1–3]. Traffic-related airborne PM_{2.5} is a complex mixture of particles and gases from gasoline and diesel engines, together with dust from wear of road surfaces, tires, and brakes [4, 5]. Airborne PM_{2.5} demonstrates an incremental capacity to penetrate into the distal airway units and potentially enter the systemic circulation with diminishing sizes. It has been suggested that the cytotoxic effects of PM_{2.5} are more associated with PM_{2.5} as a complex other than single or a few components of PM_{2.5} particles [6]. The particle sizes, charges, and combined effects of individual components of PM_{2.5} are all crucial to the adverse health impact of PM_{2.5} exposure. Studies from our group and others suggested that PM_{2.5} exposure triggers a variety of maladaptive signaling pathways in the lung, blood vessels, liver, and adipose tissues that are associated with endoplasmic reticulum (ER) stress, oxidative stress, and inflammatory responses [1, 7–12]. Moreover, we recently demonstrated an important finding that inhalation exposure to PM_{2.5} causes a NASH-like phenotype and depletion of hepatic glycogen storage in animals [1]. Through both *in vivo* and *in vitro* analyses, we revealed the signaling pathways through which PM_{2.5} exposure promotes NASH-associated activities and impairment of hepatic glucose metabolism. We identified disruption of hepatic lipid/glucose homeostasis, lobular and portal inflammation, as well as mild hepatic steatosis in the liver of the mice exposed to PM_{2.5} for 10 weeks [1]. However, the pronounced effect of PM_{2.5} exposure on modulating hepatic pathways associated with liver fibrogenesis has not been characterized.

Liver fibrosis and cirrhosis are the advanced stages of chronic liver injuries caused by chronic hepatitis viral infection, obesity, alcoholism, or autoimmune diseases. Recent studies showed that PM_{2.5} exposure activates Kupffer cells in murine liver tissues, indicating that PM_{2.5} represents a risk factor for NAFLD progression [1, 10, 13]. In this study, we used a “real-world” PM_{2.5} exposure system, “Ohio’s Air Pollution Exposure System for the Interrogation of Systemic Effects (OASIS)”, to perform whole-body exposure of mice to environmentally relevant PM_{2.5}. We demonstrate that exposure to PM_{2.5} causes a discernible phenotype of hepatic fibrosis in animals. Through both *in vivo* and *in vitro* analyses, we reveal the signaling pathways through which PM_{2.5} exposure promotes hepatic fibrogenesis-associated activities. The information from this work has important implications in the understanding and treatment of air pollution-induced liver diseases.

Materials and Methods

Animal experiments

C57BL/6 male mice of six-week-old were purchased from the Jackson Laboratories (Bar Harbor, ME), and were equilibrated for 2 weeks prior to experimental enrollment. The mice were housed in cages with regular chow or a high-fat diet (Teklad TD 88137, 42% calories from fat) in an Association for Assessment and Accreditation of Laboratory Animal Care-accredited animal housing facility. All the animal experiments were approved by the Ohio State University and the Wayne State University IACUC committee and carried out under the institutional guidelines for ethical animal use.

Exposure of animals to ambient PM_{2.5}

Mice were exposed to concentrated ambient PM_{2.5} or filtered air (FA) in the “Ohio’s Air Pollution Exposure System for the Interrogation of Systemic Effects (OASIS)” in Columbus, OH, where most of the PM_{2.5} component is attributed to long-range transport [10]. The concentrated PM_{2.5} was generated using a versatile aerosol concentration enrichment system (VACES) as we described previously [14]. Mice under the normal chow or high-fat diet were exposed to concentrated PM_{2.5} for 6 hours per day, 5 days per week for 10 weeks or 9 months [1, 10]. The control (FA) mice were exposed to an identical protocol with the exception of a high-efficiency particulate-air filter positioned in the inlet valve to remove all of the PM_{2.5} in the filtered air stream. Mice deficient in the cytosolic subunit of the nicotinamide adenine dinucleotide phosphate (NADPH) oxidase (p47phox^{-/-}) and wild-type control mice of C57BL/6 strain background (both from Jackson Laboratories) were exposure to FA or PM_{2.5} beginning at the age of 3 weeks for a duration of 10 weeks.

Histological scoring for hepatic fibrosis

Paraffin-embedded mouse liver tissue sections (5 µm) were subjected to Sirius-red or Masson’s trichrome staining for hepatic fibrosis. The histological analysis of liver fibrosis were as described previously [15, 16]. Each section was examined by a specialist who was blinded to the sample information. Hepatic fibrosis were scored according to the modified Scheuer scoring system for fibrosis and cirrhosis [16, 17]. The fibrosis stage scores were based on the 0–4 stage system: 0, none; 1, zone 3 perisinusoidal fibrosis; 2, zone 3 perisinusoidal fibrosis plus portal fibrosis; 3, perisinusoidal fibrosis, portal fibrosis, plus bridging fibrosis; and 4, cirrhosis.

Statistics

Experimental results are shown as mean ± SEM (for variation between animals or experiments). All *in vitro* experiments were repeated with biological triplicates at least three times independently. The data were analyzed and compared by paired, 2-tailed Student’s *t* tests. Multiple comparisons were compared with ANOVA and proceeded by ad hoc statistical test when necessary. Statistical tests with *p* < 0.05 were considered significant.

For a full description of materials and methods used in this work, see Supplemental Information.

Results

Inhalation exposure to PM_{2.5} induces discernible hepatic fibrosis in mice

To elucidate *in vivo* effects of PM_{2.5} exposure, male C57BL/6 mice on the normal chow or high-fat diet were exposed to concentrated ambient PM_{2.5} or FA in exposure chambers of OASIS located at Columbus, USA, where most of the PM_{2.5} is attributed to long-range transport [1, 10] (S-Figure 1). OASIS is a versatile aerosol concentration enrichment system (VACES) through which fine and ultrafine particles are concentrated and exposed to the animals in the chambers [10, 18]. It has been demonstrated that the distribution and size of concentrated PM_{2.5} collected from the exposure chamber air truly reflect that of non-concentrated PM_{2.5} present in the ambient air [14, 19]. At the same exposure site, animals were exposed to PM_{2.5} or FA for 10 weeks or 9 months in two different time periods. During the first exposure period, the ambient mean daily PM_{2.5} concentration at the study site was 6.5 µg/m³, while the mean concentration of PM_{2.5} in the exposure chamber was 74.6 µg/m³ [1]. During the second exposure period, the ambient mean daily PM_{2.5} concentration at the site was 15.8 µg/m³, and the mean concentration of PM_{2.5} in the exposure chamber was 111.0 µg/m³ [20]. Previously, we reported that the elemental composition, as measured by energy-dispersive X-ray fluorescence (ED-XRF) analysis, include alkali metals, alkaline earth metals, transition metals, poor metals, non-metals, metalloid, and halogens [10].

To evaluate effects of PM_{2.5} exposure on liver fibrosis, we first performed histological analyses with liver tissue sections of the mice exposed to PM_{2.5} or FA for 10 weeks. Sirius-red and Masson's Trichrome staining of collagen deposition revealed significant perisinusoidal fibrosis in the liver of the mice under normal chow diet exposed to PM_{2.5} (Figure 1A–B). The fibrosis grades of the PM_{2.5}-exposed mice were significantly higher than that of the FA-exposed mice (Figure 1D). We evaluated production of collagen proteins in the livers of the mice under PM_{2.5} exposure. Levels of collagen I, the major collagen protein in liver extracellular matrix, were significantly increased in the livers of the PM_{2.5}-exposed mice (Figure 1E). These results indicate a discernible effect of PM_{2.5} exposure on promoting hepatic fibrosis. Furthermore, we evaluated hepatic fibrosis in the PM_{2.5}-exposed animals under the high-fat diet. The grades of hepatic fibrosis in the animals that were simultaneously fed the high-fat diet and exposed to PM_{2.5} for 10 weeks were significantly higher than that of FA-exposed control animals (Figure 1A–B, D–E). Notably, the high-fat-fed, PM_{2.5}-exposed animals displayed advanced stages of hepatic fibrosis, including portal fibrosis and bridging fibrosis, as shown by histological analysis of collagen disposition (Figure 1A), suggesting that PM_{2.5} exposure may interact with the high-fat diet to exacerbate its effect in promoting fibrogenesis. Additionally, we examined hepatic fibrosis in the animals under the normal chow diet exposed to PM_{2.5} for 9 months. Interestingly, the hepatic fibrosis grades in the animals after 9-month PM_{2.5} exposure were only insignificantly higher than those of the FA-exposed animals (S-Figure 2A-B). This observation suggests that the animals may possess adaptation mechanisms to attenuate the effect of a single environmental risk factor during the chronic PM_{2.5} exposure.

Next, we examined expression of α-smooth muscle actin (α-SMA), a prominent marker for activation of hepatic stellate cells (HSC) and fibrosis progression [21], in the livers of PM_{2.5}-

or FA-exposed mice under the normal chow or high-fat diet. Immunohistochemical analysis showed markedly increased α -SMA staining in the mouse liver tissues upon PM_{2.5} exposure, suggesting a strong effect of PM_{2.5} exposure on HSC activation (Figure 1C). In hepatic fibrosis, the release of latent transforming growth factor β (TGF β) stimulates HSC to produce collagens, a key event of hepatic fibrogenesis [22, 23]. Enzyme-linked immunosorbent assay (ELISA) indicated that serum levels of activated TGF β 1 in the mice exposed to PM_{2.5} were significantly higher than those of the FA-exposed mice (Figure 1F). Gene expression analysis confirmed higher expression levels of *Tgfb1* mRNA in the livers of mice exposed to PM_{2.5} (Figure 1G). Together, these results implicate that TGF β , the inflammatory trigger of hepatic fibrosis, is up-regulated upon PM_{2.5} challenge.

Exposure to PM_{2.5} stimulates TGF β release by macrophages and collagen production by HSC

In the liver, fibrogenesis is a coordinated process that involves multiple specialized cell types, including Kupffer cells (resident macrophages), Ito cells (quiescent adipocytes), HSC, and extracellular matrix [22]. Upon liver injuries or chronic stress, Ito cells can be activated and differentiated into myofibroblastic HSC with decreased PPAR γ expression and fat-storing function [24, 25]. In this process, TGF β produced by inflammatory cells facilitates the differentiation of myofibroblastic HSC, which is specialized in producing extracellular matrix proteins, especially collagens, to promote hepatic fibrogenesis [22, 23]. It has been reported that three major liver cell types, Kupffer cells, HSC, and hepatocytes, can produce TGF β in liver pathogenesis [26, 27]. Previously we demonstrated that PM_{2.5} exposure activates Kupffer cells in animal models [1]. Numbers of activated macrophages and induction of macrophage-associated inflammatory cytokine genes, including *TGF β 1*, *IL1 β* , *IL6*, *TNF α* , *IL8*, *CCL2*, *CCL3*, and *Gro1*, were increased in the liver of PM_{2.5}-exposed mice (S-Figure 3A–D). To define the target liver cell types that produce TGF β under PM_{2.5} exposure, we exposed mouse primary hepatocytes, macrophage cell line RAW264.7, and LX-2, a human HSC cell line that retains the key features of HSC and has been used to study hepatic fibrosis and liver disease [28], to PM_{2.5} particles. In response to PM_{2.5} challenge, levels of activated TGF β in the culture medium from RAW264.7 cells, but not hepatocytes or LX-2 cells, were increased in a time-dependent manner (Figure 2A). Gene expression analysis confirmed that expression of the mRNAs encoding TGF β 1, TGF β 2, and TGF β 3 in RAW264.7 cells was significantly increased upon PM_{2.5} exposure (Figure 2B). These results suggest that macrophage is the major cell type that produces TGF β under PM_{2.5} exposure.

We further assessed the effects of PM_{2.5} on fibrogenesis-associated signaling in HSC. LX-2 cells were cultured in the conditioned medium from the macrophage cell line RAW264.7 exposed to PM_{2.5} or vehicle for 12 and 24 hours, respectively. Upon PM_{2.5} exposure, phosphorylation of SMAD3, a key mediator of TGF β -triggered fibrotic response [29], was significantly increased in LX-2 cells in a time-dependent manner (Figure 2C). Correlated to the phosphorylation of SMAD3, expression levels of both mRNAs and proteins of collagen I and α -SMA were increased in LX-2 cells incubated with the conditioned media from PM_{2.5}-exposed macrophages (Figure 2D–E, S-Figure 5). Additionally, we visualized production of collagen I and collagen IV in LX-2 cells upon PM_{2.5} challenge through immunofluorescent analysis. LX-2 cells cultured in the conditioned medium from PM_{2.5}-exposed RAW264.7

cells produced much more collagen I and collagen IV proteins than those cultured in the control medium (Figure 2F and S-Figure 4), thus confirming the effect of PM_{2.5} exposure on collagen production by HSC. Further, to verify whether the PM_{2.5}-induced collagen production from HSC depends on TGFβ signaling, we incubated LX2 cells with the specific TGF receptor (TGFR) inhibitor SB431542 prior to the culture with the conditioned medium from PM_{2.5}- or vehicle-exposed RAW264.7 cells. Under PM_{2.5}-exposed conditioned medium, pre-treatment of SB431542 significantly reduced both mRNA and protein levels of collagen I in LX2 cells (S-Figure 6), suggesting a crucial role of TGFβ signaling in PM_{2.5}-induced hepatic fibrogenesis as well as the effectiveness of TGFβ receptor antagonist SB431542 in suppressing PM_{2.5}-induced hepatic fibrosis.

Exposure to PM_{2.5} represses PPARγ in HSC

It is known that expression of PPARγ in HSC is closely associated with fibrosis in the liver under injuries or chronic stress [24, 25]. The decrease in expression of PPARγ enables the quiescent adipocytes (Ito cells) to be activated and further differentiated into myofibroblastic HSC [24, 25]. Previously, we showed that inhalation exposure to PM_{2.5} reduces expression of PPARγ and PPARα in liver tissues [1]. However, we have not determined whether PM_{2.5} exposure modulates PPARγ expression in stellate cells. To determine whether PM_{2.5} exposure can modulate PPARγ expression in HSC, we examined levels of PPARγ in the HSC cell line LX-2 upon PM_{2.5} challenge. LX-2 cells were cultured in the conditioned medium from macrophage cell line RAW264.7 exposed to PM_{2.5} for 12 or 24 hrs. Upon exposure to the conditioned medium, both protein and mRNA levels of PPARγ were gradually decreased in LX-2 cells in a manner that depends on the PM_{2.5} exposure time of RAW264.7 cells (Figure 3A–B).

Pioglitazone is a commonly-used PPARγ agonist to prevent inflammation, fibrosis, and insulin resistance in type II diabetes patient by increasing PPARγ levels [30]. To test whether Pioglitazone can prevent PM_{2.5}-triggered down-regulation of PPARγ in HSC, LX-2 cells were incubated with Pioglitazone for 48hr followed by incubation with the conditioned medium from PM_{2.5}-exposed RAW264.7 cells. The pre-treatment of pioglitazone at the concentration of 1μM can partially rescue the down-regulation of *PPARγ1* and *PPARγ2* mRNA expression in the LX-2 cells cultured in the conditioned media from PM_{2.5}-exposed RAW264.7 cells (Figure 3C–D). Interestingly, when the concentration of pioglitazone was increased to 2.5μM, the pioglitazone pre-treatment was effective in increasing expression of *PPARγ2*, but not *PPARγ1*, in LX-2 cells. Immunoblotting analysis confirmed that pioglitazone treatment at the concentration of 1μM can rescue the down-regulation of PPARγ protein levels by PM_{2.5} in LX-2 cells (Figure 3E). These results imply the potential role of the PPARγ antagonist pioglitazone in preventing PM_{2.5}-induced hepatic fibrogenesis by attenuating PM_{2.5}-induced PPARγ down-regulation.

PM_{2.5}-induced hepatic fibrosis relies on NADPH oxidase

We explored potential involvements of cell stress sensors in PM_{2.5}-induced hepatic fibrosis. It is known that NADPH oxidase (NOX) generates large amounts of superoxide anions in phagocytes and plays a key role in immune defense [31]. Kupffer cells highly express NOX and generate high amounts of reactive oxygen species (ROS) in response to early liver

injuries [32]. Upon cellular stress, neutrophil cytosolic factor 1 (NCF1 or p47phox), a key regulatory subunit of NOX, is phosphorylated and translocate to the cell membrane to form the active NOX. To assess the involvement of NADPH oxidase in experimental liver fibrosis, we exposed p47phox knockout (p47phox^{-/-}) and wild-type control mice to PM_{2.5} or FA for 10 weeks. Upon PM_{2.5} exposure, p47phox^{-/-} mice exhibited significantly attenuated liver fibrosis, compared to the wild-type counterparts (Figure 4A–B), suggesting that NOX plays a major role in mediating the action of PM_{2.5} exposure in hepatic fibrogenesis. Consistent with the hepatic fibrosis staining result, expression levels of *Collagen 1* mRNA in the liver tissues of the p47phox^{-/-} mice were dramatically decreased, compared to that of the control mice, under PM_{2.5} exposure (Figure 4C).

Next, we examined production of ROS, an important trigger of hepatic fibrosis [33], in the liver tissues of p47phox^{-/-} and control mice after PM_{2.5} exposure. While inhalation exposure to PM_{2.5} significantly induced ROS in the liver tissues of the wild-type control mice, PM_{2.5}-triggered ROS production was significantly reduced in the p47phox^{-/-} mice (Figure 4D–E). Additionally, we examined hepatic steatosis in the p47phox^{-/-} and wild-type control mice after PM_{2.5} exposure (Figure 4F). Consistent with our early finding, PM_{2.5} exposure lead to hepatic lipid accumulation in the wild-type mice. However, hepatic steatosis was relieved in the PM_{2.5}-exposed p47phox^{-/-} mice, compared to that of wild-type mice under PM_{2.5} exposure (Figure 4F), suggesting a critical role of NOX in mediating PM_{2.5}-induced hepatic steatosis. Furthermore, we examined expression of PPAR γ and TGF β 1 in the livers of p47phox^{-/-} and control mice under PM_{2.5} exposure. While PM_{2.5} exposure repressed expression of *PPAR γ* mRNA in the wild-type mice, expression of *PPAR γ* in the p47phox^{-/-} mouse livers was not suppressed by PM_{2.5} exposure (Figure 4G). Indeed, the levels of *PPAR γ* mRNA were even increased in the livers of PM_{2.5}-exposed p47phox^{-/-} mice, compared to the PM_{2.5}-exposed wild-type mice or FA-exposed p47phox^{-/-} mice. Moreover, PM_{2.5} exposure was not able to increase expression of *Tgf β 1* mRNA in the p47phox^{-/-} liver (S-Figure 7). Together, these results suggested that NOX plays an important role in mediating the action of PM_{2.5} exposure in suppressing PPAR γ and stimulating TGF β 1 expression in the liver.

Discussion

In this study, we demonstrate that inhalation exposure to PM_{2.5} represents a significant risk factor to hepatic fibrosis. Previously, we revealed important roles of ER stress, oxidative stress, and inflammation in liver pathogenesis under PM_{2.5} exposure [1, 10]. Our works demonstrated that animals under PM_{2.5} exposure displayed a NASH-like phenotype, reduction of hepatic glycogen storage, and hepatic insulin resistance under normal chow diet [1]. The current work extends our prior observations on the link between air-pollution exposure and liver pathogenesis. While PM_{2.5} exposure alone can cause mild but discernable hepatic fibrosis, PM_{2.5} can interact with another health risk factor, the high-fat diet, to facilitate advanced stages of hepatic fibrosis.

Hepatic inflammation is a major contributing factor to the development of liver fibrosis. Our study showed that inhalation exposure to PM_{2.5} induces TGF β production in mouse liver, presumably from Kupffer cells, which subsequently stimulates SMAD3 signaling and

Collagen expression in HSCs (Figures 1–2). As suggested by our previous studies, systemic inflammation through circulating inflammatory cytokines, macrophage or neutrophil infiltration, and direct stimulation of Kupffer cells by PM_{2.5} particles delivered to the liver can all potentially promote hepatic inflammation [1, 10]. Therefore, systemic inflammation and infiltrated leukocytes, in addition to Kupffer cells, may also be involved in facilitating hepatic fibrosis through the TGFβ-SMAD3-Collagen regulatory axis. Another important event linking to hepatic fibrosis is the down-regulation of PPARγ by PM_{2.5} exposure in HSC. In the liver, PPARγ plays important roles in anti-inflammatory response and energy homeostasis associated with HSC, Kupffer cells, and hepatocytes [34]. In particular, the differentiation of HSCs from Ito cells is inversely correlated with PPARγ levels [24]. Therefore, the down-regulation of PPARγ in HSC could be important to the progression of hepatic fibrogenesis in PM_{2.5}-exposed mice (Figure 3). Additionally, hepatic steatosis developed under PM_{2.5} exposure, partially due to repression of PPARα and PPARγ [1], may also contribute to the progression of liver fibrosis. Based on these scenarios, delineating which inflammatory pathways, either systemic or local, are relatively important in promoting hepatic fibrogenesis, and defining the extent to which hepatic inflammation or steatosis contributes to liver fibrosis under PM_{2.5} exposure, are interesting subjects to be investigated in the future.

Our study demonstrated that PM_{2.5}-induced hepatic steatosis relies on NOX activity. We previously reported a critical role of NOX in mediating oxidative stress, as p47phox^{-/-} animals appeared to be protective from PM_{2.5}-mediated insulin resistance and inflammation [20, 35]. Studies from other groups showed that NOX is critically involved in hepatic fibrosis induced by angiotensin II, bile duct ligation, or methionine-choline-deficient diet [36, 37]. Our work with PM_{2.5} exposure provides new evidence that NOX is essential for hepatic fibrosis under real-world environmental stress. NOX generates large amounts of ROS in phagocytic cells, and ROS is known to play an important role in hepatic fibrosis [31, 32]. Under PM_{2.5} exposure, p47phox^{-/-} mice displayed significantly reduced ROS production and hepatic fibrosis (Figure 4). Importantly, PM_{2.5}-induced down-regulation of PPARγ and up-regulation of TGFβ1 were attenuated in the livers of p47phox^{-/-} mice (Figure 4G, S-Figure 7), suggesting that NOX plays a major role in mediating PM_{2.5}-triggered fibrogenesis through modulating PPARγ and TGFβ signaling.

The significance of our study needs to be placed in the context of real-world PM_{2.5} exposure. The PM_{2.5} concentration in the animal exposure chambers was approximately 10-time of daily ambient PM_{2.5} concentration in most US and European cities. In the developing countries, such as China, India, and Latin American, where the daily PM_{2.5} levels range from 100 to 200 μg/m³ (approximately 10–20 fold higher than those in major U.S. cities) [38], the detrimental effects of PM_{2.5} exposure on public health have been grossly underestimated. Even in U.S. or European countries, the prevalence of metabolic syndrome was increased with increasing PM_{2.5} concentrations, as evidenced by a 1% increase in diabetes prevalence seen with a 10 μg/m³ increase in PM_{2.5} exposure [39]. Therefore, the PM_{2.5} levels at high ranges, as obtained through our experimental exposure system, not only recapitulate true air pollution environment in the developing countries but also can be translated into cumulative exposures in U.S. or European countries. Our studies suggest that liver is an important target organ and a key player in pathophysiology under

PM_{2.5} exposure. This finding has important implications in the medical care from the prevention to treatment of systemic diseases associated with air pollution.

Supplementary Material

Refer to Web version on PubMed Central for supplementary material.

Acknowledgments

Portions of this work were supported by National Institutes of Health (NIH) grants DK090313 and ES017829 to KZ, American Heart Association Grants 0635423Z and 09GRNT2280479 to KZ, NIH grant ES018900 to QS, and NIH grants R01ES019616, R01ES017290, and R01ES015146 to SR. We thank Dr. Scott Friedman for kindly providing LX-2 cells.

Abbreviations

PM	ambient particulate matter
PM_{2.5}	PM with aerodynamic diameter less than 2.5 μm
FA	filtered air
OASIS	Ohio's Air Pollution Exposure System for the Interrogation of Systemic Effects
PPAR	peroxisome proliferator-activated receptor
TGFβ	transforming growth factor β
HSC	hepatic stellate cells
p47phox	Neutrophil cytosolic factor 1
NOX	NADPH peroxidase
ROS	reactive oxygen species

References

1. Zheng Z, Xu X, Zhang X, Wang A, Zhang C, Huttemann M, et al. Exposure to ambient particulate matter induces a NASH-like phenotype and impairs hepatic glucose metabolism in an animal model. *J Hepatol.* 2013; 58:148–154. [PubMed: 22902548]
2. Liu C, Xu X, Bai Y, Wang TY, Rao X, Wang A, et al. Air pollution-mediated susceptibility to inflammation and insulin resistance: influence of CCR2 pathways in mice. *Environ Health Perspect.* 2014; 122:17–26. [PubMed: 24149114]
3. Sun L, Liu C, Xu X, Ying Z, Maiseyeu A, Wang A, et al. Ambient fine particulate matter and ozone exposures induce inflammation in epicardial and perirenal adipose tissues in rats fed a high fructose diet. *Part Fibre Toxicol.* 2013; 10:43. [PubMed: 23968387]
4. Alfaro-Moreno E, Martinez L, Garcia-Cuellar C, Bonner JC, Murray JC, et al. Biologic effects induced in vitro by PM10 from three different zones of Mexico City. *Environ Health Perspect.* 2002; 110:715–720. [PubMed: 12117649]
5. Soukup JM, Becker S. Human alveolar macrophage responses to air pollution particulates are associated with insoluble components of coarse material, including particulate endotoxin. *Toxicology and applied pharmacology.* 2001; 171:20–26. [PubMed: 11181108]

6. Brook RD, Franklin B, Cascio W, Hong Y, Howard G, Lipsett M, et al. Air pollution and cardiovascular disease: a statement for healthcare professionals from the Expert Panel on Population and Prevention Science of the American Heart Association. *Circulation*. 2004; 109:2655–2671. [PubMed: 15173049]
7. Xu X, Liu C, Xu Z, Tzan K, Wang A, Rajagopalan S, et al. Altered adipocyte progenitor population and adipose-related gene profile in adipose tissue by long-term high-fat diet in mice. *Life sciences*. 2012; 90:1001–1009. [PubMed: 22683431]
8. Kampfrath T, Maiseyeu A, Ying Z, Shah Z, Deuliis JA, Xu X, et al. Chronic fine particulate matter exposure induces systemic vascular dysfunction via NADPH oxidase and TLR4 pathways. *Circulation research*. 2011; 108:716–726. [PubMed: 21273555]
9. Wang G, Rajagopalan S, Sun Q, Zhang K. Real-world exposure of airborne particulate matter triggers oxidative stress in an animal model. *Int J Physiol Pathophysiol Pharmacol*. 2010; 2:64–68. [PubMed: 21383899]
10. Laing S, Wang G, Briazova T, Zhang C, Wang A, Zheng Z, et al. Airborne particulate matter selectively activates endoplasmic reticulum stress response in the lung and liver tissues. *Am J Physiol Cell Physiol*. 2010; 299:C736–C749. [PubMed: 20554909]
11. Mendez R, Zheng Z, Fan Z, Rajagopalan S, Sun Q, Zhang K. Exposure to fine airborne particulate matter induces macrophage infiltration, unfolded protein response, and lipid deposition in white adipose tissue. *Am J Transl Res*. 2013; 5:224–234. [PubMed: 23573366]
12. Chen LC, Quan C, Hwang JS, Jin X, Li Q, Zhong M, et al. Atherosclerosis lesion progression during inhalation exposure to environmental tobacco smoke: a comparison to concentrated ambient air fine particles exposure. *Inhalation toxicology*. 2010; 22:449–459. [PubMed: 20235771]
13. Tan HH, Fiel MI, Sun Q, Guo J, Gordon RE, Chen LC, et al. Kupffer cell activation by ambient air particulate matter exposure may exacerbate non-alcoholic fatty liver disease. *J Immunotoxicol*. 2009
14. Maciejczyk P, Zhong M, Li Q, Xiong J, Nadziejko C, Chen LC. Effects of subchronic exposures to concentrated ambient particles (CAPs) in mice. II. The design of a CAPs exposure system for biometric telemetry monitoring. *Inhalation toxicology*. 2005; 17:189–197. [PubMed: 15804936]
15. Zheng Z, Zhang C, Zhang K. Measurement of ER stress response and inflammation in the mouse model of nonalcoholic fatty liver disease. *Methods Enzymol*. 2011; 489:329–348. [PubMed: 21266239]
16. Brunt EM. Nonalcoholic steatohepatitis: definition and pathology. *Seminars in liver disease*. 2001; 21:3–16. [PubMed: 11296695]
17. Kleiner DE, Brunt EM, Van Natta M, Behling C, Contos MJ, Cummings OW, et al. Design and validation of a histological scoring system for nonalcoholic fatty liver disease. *Hepatology*. 2005; 41:1313–1321. [PubMed: 15915461]
18. Ying Z, Yue P, Xu X, Zhong M, Sun Q, Mikolaj M, et al. Air pollution and cardiac remodeling: a role for RhoA/Rho-kinase. *Am J Physiol Heart Circ Physiol*. 2009; 296:H1540–H1550. [PubMed: 19286943]
19. Chen LC, Nadziejko C. Effects of subchronic exposures to concentrated ambient particles (CAPs) in mice. V. CAPs exacerbate aortic plaque development in hyperlipidemic mice. *Inhalation toxicology*. 2005; 17:217–224. [PubMed: 15804939]
20. Xu X, Yavar Z, Verdin M, Ying Z, Mihai G, Kampfrath T, et al. Effect of early particulate air pollution exposure on obesity in mice: role of p47phox. *Arterioscler Thromb Vasc Biol*. 2010; 30:2518–2527. [PubMed: 20864666]
21. Akpolat N, Yahsi S, Godekmerdan A, Yalniz M, Demirbag K. The value of alpha-SMA in the evaluation of hepatic fibrosis severity in hepatitis B infection and cirrhosis development: a histopathological and immunohistochemical study. *Histopathology*. 2005; 47:276–280. [PubMed: 16115228]
22. Safadi R, Friedman SL. Hepatic fibrosis--role of hepatic stellate cell activation. *Med Gen Med*. 2002; 4:27.

23. Roth S, Gong W, Gressner AM. Expression of different isoforms of TGF-beta and the latent TGF-beta binding protein (LTBP) by rat Kupffer cells. *J Hepatol.* 1998; 29:915–922. [PubMed: 9875638]
24. Miyahara T, Schrum L, Rippe R, Xiong S, Yee HF Jr, Motomura K, et al. Peroxisome proliferator-activated receptors and hepatic stellate cell activation. *J Biol Chem.* 2000; 275:35715–35722. [PubMed: 10969082]
25. Hautekeete ML, Geerts A. The hepatic stellate (Ito) cell: its role in human liver disease. *Virchows Archiv.* 1997; 430:195–207. [PubMed: 9099976]
26. Ankoma-Sey V. Hepatic Regeneration-Revisiting the Myth of Prometheus. *News in physiological sciences.* 1999; 14:149–155. [PubMed: 11390841]
27. Sakata R, Ueno T, Nakamura T, Ueno H, Sata M. Mechanical stretch induces TGF-beta synthesis in hepatic stellate cells. *Eur J Clin Invest.* 2004; 34:129–136. [PubMed: 14764076]
28. Xu L, Hui AY, Albanis E, Arthur MJ, O'Byrne SM, Blaner WS, et al. Human hepatic stellate cell lines, LX-1 and LX-2: new tools for analysis of hepatic fibrosis. *Gut.* 2005; 54:142–151. [PubMed: 15591520]
29. Flanders KC. Smad3 as a mediator of the fibrotic response. *Int J Exp Pathol.* 2004; 85:47–64. [PubMed: 15154911]
30. Gillies PS, Dunn CJ. Pioglitazone. *Drugs.* 2000; 60:333–343. discussion 344-335. [PubMed: 10983737]
31. Babior BM, Lambeth JD, Nauseef W. The neutrophil NADPH oxidase. *Arch. Biochem. Biophys.* 2002; 397:342–344. [PubMed: 11795892]
32. Wheeler MD, Kono H, Yin M, Nakagami M, Uesugi T, Arteel GE, et al. The role of Kupffer cell oxidant production in early ethanol-induced liver disease. *Free Radic Biol Med.* 2001; 31:1544–1549. [PubMed: 11744328]
33. Parola M, Robino G. Oxidative stress-related molecules and liver fibrosis. *J Hepatol.* 2001; 35:297–306. [PubMed: 11580156]
34. Feige JN, Gelman L, Michalik L, Desvergne B, Wahli W. From molecular action to physiological outputs: peroxisome proliferator-activated receptors are nuclear receptors at the crossroads of key cellular functions. *Prog Lipid Res.* 2006; 45:120–159. [PubMed: 16476485]
35. Ying Z, Kampfrath T, Thurston G, Farrar B, Lippmann M, Wang A, et al. Ambient particulates alter vascular function through induction of reactive oxygen and nitrogen species. *Toxicological sciences.* 2009; 111:80–88. [PubMed: 19182107]
36. Bataller R, Schwabe RF, Choi YH, Yang L, Paik YH, Lindquist J, et al. NADPH oxidase signal transduces angiotensin II in hepatic stellate cells and is critical in hepatic fibrosis. *J Clin Invest.* 2003; 112:1383–1394. [PubMed: 14597764]
37. De Minicis S, Seki E, Paik YH, Osterreicher CH, Kodama Y, Kluwe J, et al. Role and cellular source of nicotinamide adenine dinucleotide phosphate oxidase in hepatic fibrosis. *Hepatology.* 2010; 52:1420–1430. [PubMed: 20690191]
38. Tao JG J, Zhang L, Zhang R, Che H, Zhang Z, Lin Z, Jing J, Cao J, Hsu S-C. PM2.5 pollution in a megacity of southwest China: source apportionment and implication. *Atmos Chem Phys.* 2014; 14:20.
39. Pearson JF, Bachireddy C, Shyamprasad S, Goldfine AB, Brownstein JS. Association between fine particulate matter and diabetes prevalence in the U.S. *Diabetes care.* 2010; 33:2196–2201. [PubMed: 20628090]

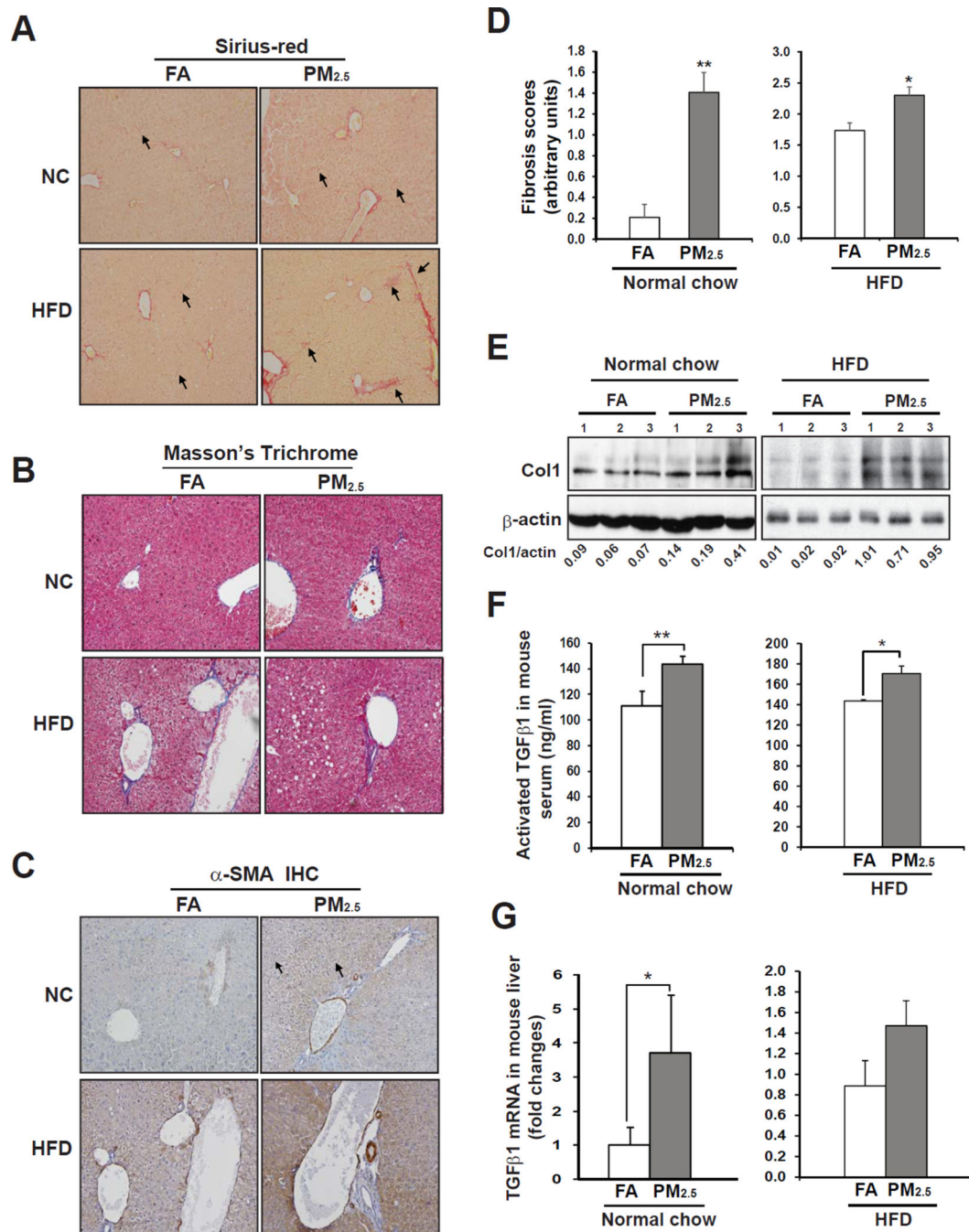


Figure 1. PM_{2.5} exposure induces hepatic fibrosis in mouse liver

(A–B) Sirius-red staining of hepatic collagen deposition (A) and Masson's Trichrome Staining of collagen fiber (B) in formalin-fixed liver tissue sections from C57BL/6 mice under the normal chow (NC) or high-fat diet (HFD) exposed to FA or PM_{2.5} for 10 weeks. Magnifications: 200×. The arrows point out areas of hepatic fibrosis. (C) Immunohistochemical staining of the hepatic stellate cell surface marker α-SMA in the liver tissue sections from the NC- or HFD-fed mice exposed to FA or PM_{2.5} for 10 weeks. Magnifications: 600×. (D) Hepatic fibrosis grades of the mice exposed to PM_{2.5} or FA for 10

weeks. Hepatic fibrosis grades were determined based on the histological analyses of Sirius-red staining of collagens, according to the Scheuer scoring system for fibrosis and cirrhosis [16, 17]. Data are shown as mean \pm SEM (n= 8 FA- or 9 PM_{2.5}-exposed animals). **(E)** Immunoblotting analysis of collagen I (Col1) in the liver tissue from the mice exposed to PM_{2.5} or FA. The values below gel images represent quantification of Col1 protein signal intensities after normalization to those of β -actin. **(F)** Serum levels of activated TGF β 1 (determined by ELISA) in the mice exposed to PM_{2.5} or FA. For A–B, Each bar denotes the mean \pm SEM (n= 3). **(G)** Quantitative real-time PCR (qRT-PCR) analysis of expression levels of the *Tgf β 1* mRNA in the livers of the mice exposed to PM_{2.5} or FA for 10 weeks. Fold changes of mRNA levels were shown by comparing to the FA-exposed control mice. From B–G, * $p < 0.05$; ** $p < 0.01$.

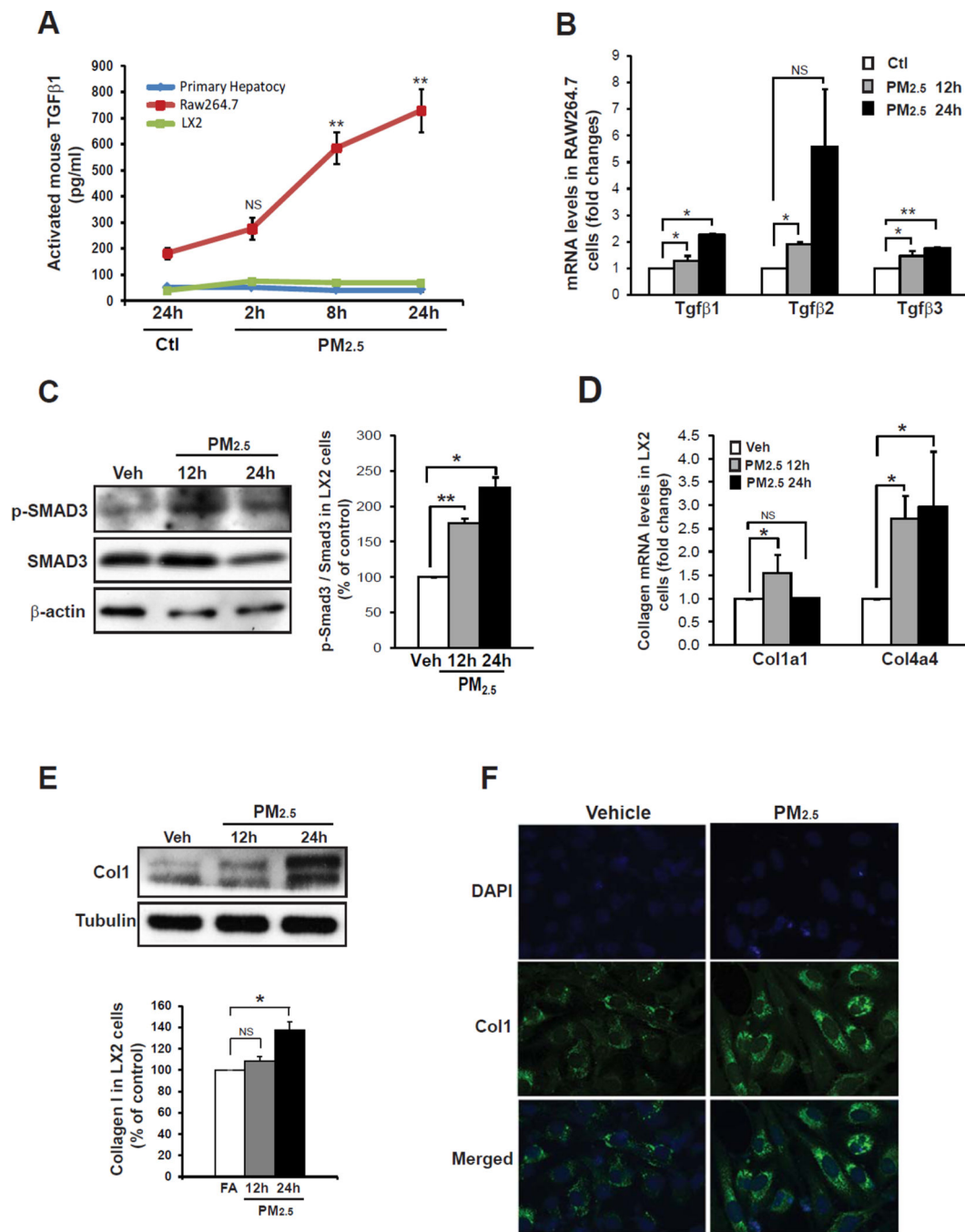


Figure 2. Exposure to PM_{2.5} stimulates TGFβ signaling in macrophages and collagen production in HSC

(A) Levels of secreted TGFβ1 in primary hepatocytes, RAW264.7 cells, and LX-2 cells upon the challenge of PM_{2.5} (5 μg/ml) for different time intervals as indicated. The levels of TGFβ1 in the culture medium were determined by ELISA and presented after normalization to cell numbers. Each time point represents the mean ± SEM (n=3 biological replicates). (B) qRT-PCR analysis of expression levels of the *Tgfβ1*, *Tgfβ2*, and *Tgfβ3* mRNAs in RAW264.7 cells challenged with PM_{2.5} for different time intervals as indicated. Fold

changes of mRNA levels were shown by comparing to the vehicle (PBS)-treated controls. Each bar represents the mean \pm SEM (n=3 biological replicates). (C) Immunoblotting analysis of total and phosphorylated SMAD3 in LX-2 cells cultured in the conditioned medium from RAW264.7 cells exposed to PM_{2.5} for 12 or 24 hours. The graph beside the images showed fold changes of phosphorylated SMAD3 levels after normalization to total SMAD3 levels. Each bar denotes the mean \pm SEM (n=3 biological replicates). (D) qRT-PCR analysis of expression levels of the *Collagen 1 α 1* (*Col1 α 1*) and *Collagen 4 α 4* (*Col4 α 4*) mRNA in LX-2 cells cultured in the conditioned medium from RAW264.7 cells exposed to PM_{2.5} for 12 or 24 hours. LX-2 cells were incubated with the conditioned medium for 36 hours before subjected to the real-time RT-PCR analysis. Fold changes of mRNA are shown by comparing to the vehicle control. Each bar denotes the mean \pm SEM (n=3 biological replicates). (E) Immunoblotting analysis of Col1 protein levels in LX-2 cells cultured in the conditioned medium from RAW264.7 cells exposed to PM_{2.5} for 12 or 24 hours. The graph beside the images showed fold changes of Collagen protein levels after normalization to those of Tubulin. Each bar denotes the mean \pm SEM (n=3 biological replicates). From A–E, * $p < 0.05$; ** $p < 0.01$. (F) Immunofluorescent analysis of Col1 production in the LX-2 cells cultured in the conditioned medium from RAW264.7 cells exposed to PM_{2.5} for 10 hours. LX-2 cells were incubated with the conditioned medium for 36 hours before subjected to the immunofluorescent analysis. LX-2 cells were cultured in the conditioned medium from RAW264.7 cells exposed to PBS (vehicle) as the control. The nucleus was stained with DAPI. The experiments were repeated 3 times, and representative images were shown.

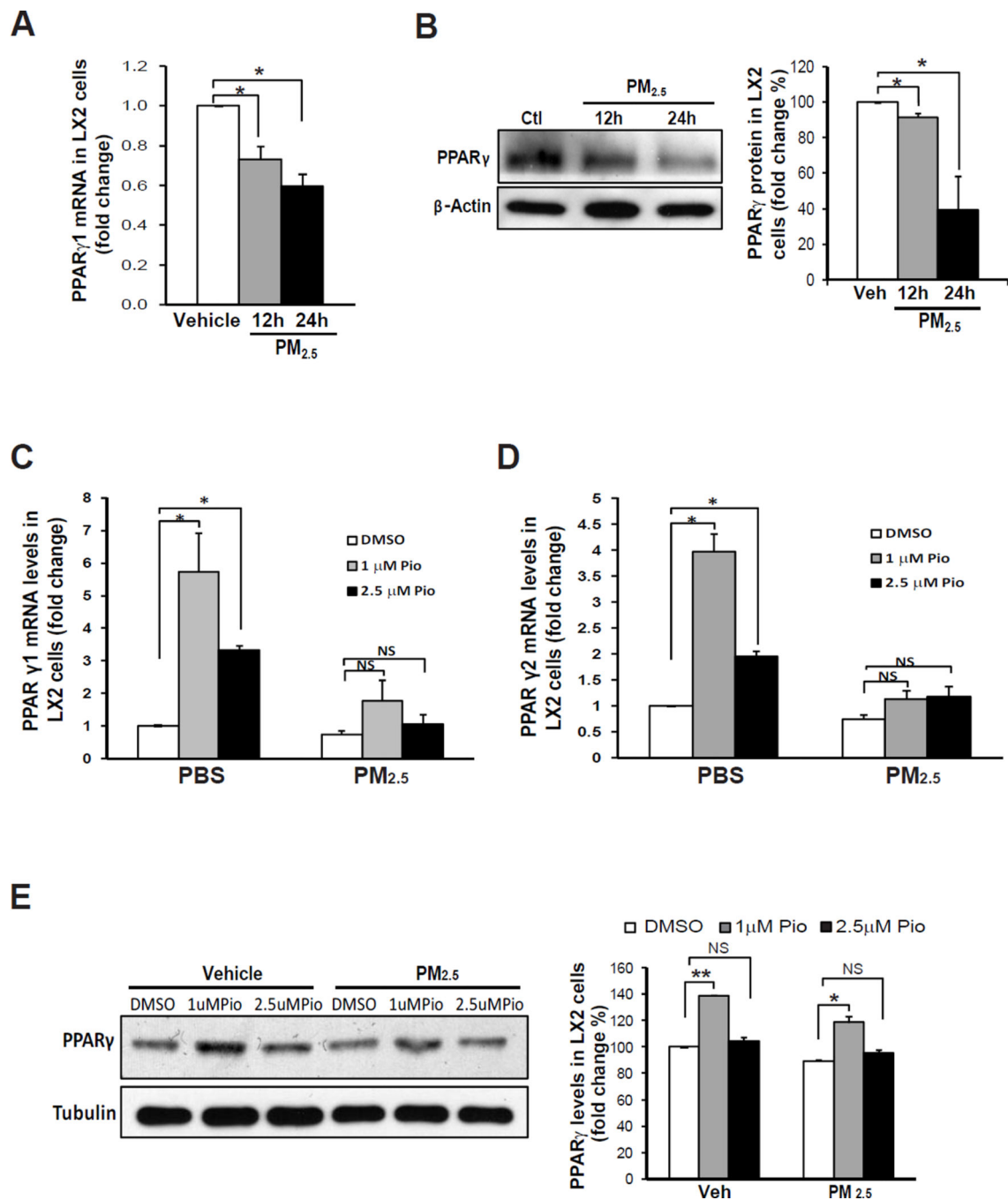


Figure 3. PM_{2.5} exposure down-regulates expression of PPAR γ in HSC

(A) Quantitative real-time PCR analysis of expression levels of *PPAR γ 1* mRNA in LX-2 cells cultured in the conditioned medium from RAW264.7 cells exposed to PM_{2.5} for 12 or 24 hours. Fold changes of mRNA are shown by comparing to the vehicle control. Each bar denotes the mean \pm SEM (n=3 biological replicates). (B) Immunoblotting analysis of PPAR γ levels in LX-2 cells cultured in the conditioned media from RAW264.7 cells exposed to PM_{2.5} for 12 or 24 hours. LX-2 cells were incubated with the conditioned medium for 36 hours before subjected to immunoblotting analysis. LX-2 cells were cultured

in the conditioned medium from RAW264.7 cells exposed to PBS for 24 hours as the control. The graph beside the images shows fold changes of PPAR γ protein levels in LX-2 cells. The fold changes of PPAR γ in PM_{2.5}-exposed LX2 cells were determined by normalizing to the PPAR γ signal intensities in PM_{2.5}-exposed LX2 cells to that of vehicle-exposed LX2 cells. (C–E) Pre-treatment of Pioglitazone (Pio) prevents PM_{2.5}-induced down-regulation of PPAR γ in HSC. LX2 cells were cultured in the presence of Pio at the concentration of 1 or 2.5 μ M for 48 hours before they were incubated with the conditioned medium from RAW264.7 cell exposed to PM_{2.5} (50 μ g/ml) for 14 hours. LX2 were incubated with the conditioned medium for 36 hours in the presence of Pio, and then subjected to extraction of RNAs and proteins for qRT-PCR analyses of *PPAR γ 1* and *PPAR γ 2* mRNA levels (C–D) and Western blot analysis of PPAR γ protein levels (E). LX2 cells treated with vehicles (DMSO, the vehicle for Pio treatment; and PBS, the vehicle for PM_{2.5}). The fold changes of *PPAR γ* mRNA levels in PM_{2.5}- and/or Pio-treated cells were determined by normalizing to *PPAR γ* levels in vehicle-treated cells. Each bar denotes the mean \pm SEM (n=3 biological replicates). The graph beside the images (panel E) showed fold changes of PPAR γ levels in LX-2 cells. The fold changes of PPAR γ in the Pio-treated LX2 cells were determined by comparing the normalized PPAR γ signal intensities in the Pio-treated LX2 cells to that in the vehicle-treated LX2 cells (100%). * P 0.05, ** P 0.01.

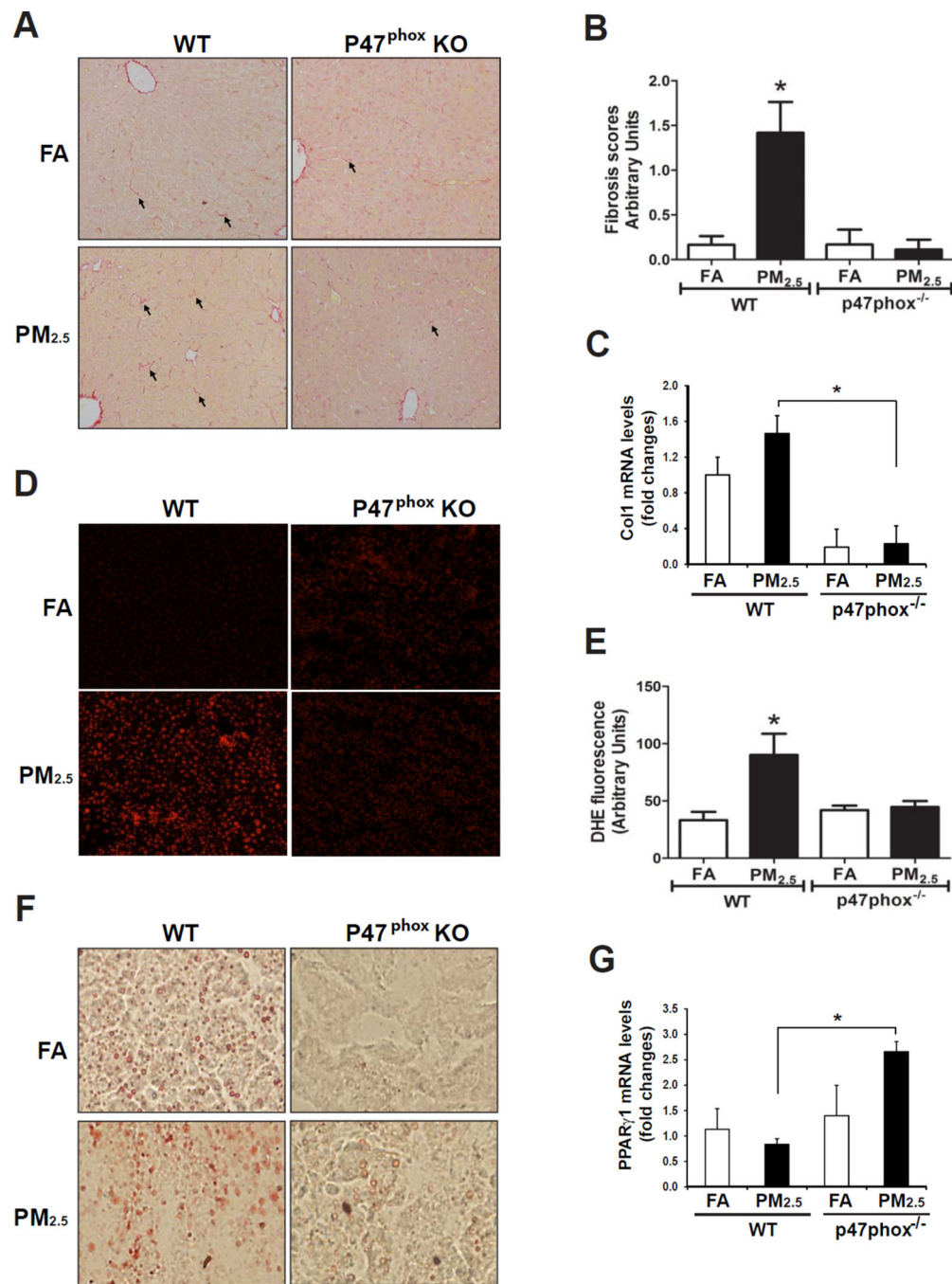


Figure 4. Hepatic fibrosis under PM_{2.5} exposure relies on NOX activity

(A) Histological analysis of hepatic collagen deposition (Sirius-red staining) in formalin-fixed liver tissue sections from p47phox^{-/-} and wild-type control mice exposed to FA or PM_{2.5} for 10 weeks. Magnifications: 200×. The arrows point out areas of hepatic fibrosis. (B) Hepatic fibrosis grades of the p47phox^{-/-} and control mice exposed to PM_{2.5} or FA. Hepatic fibrosis grades were determined based on the histological analyses of Sirius-red staining of collagens, according to the Scheuer scoring system for fibrosis and cirrhosis [16, 17]. Data are shown as mean ± SEM (n= 4 animals per group). (C) qRT-PCR analysis of

expression levels of *Col1* mRNA in p47phox^{-/-} and control mice exposed to FA or PM_{2.5} for 10 weeks. Fold changes of mRNA are shown by normalizing mRNA levels to that of the FA-exposed control animals. Each bar denotes the mean ± SEM (n=3 animals per group). **(D)** DHE staining of ROS signals in the liver tissue sections from the mice exposed to FA or PM_{2.5}. The oxidative red fluorescence was detected by a Zeiss fluorescence microscope. Magnification: 400×. **(E)** Quantification of DHE-stained ROS signals in the PM_{2.5}- and FA-exposed p47phox^{-/-} and control mice. DHE signals were quantified by counting the number of positive stained nuclei in 8 random fields. Microscopic interference contrast was used to exclude positive signals from non-cell origin. The percentages of DHE-positive nuclei (compared to total nuclei) were shown. Data are shown as mean ± SEM (n= 4 animals per group). * *P*<0.05. **(F)** Oil-red O staining of hepatic lipid droplets in the livers of p47phox^{-/-} and wild-type control mice exposed to FA or PM_{2.5} for 10 weeks (magnifications: 200×). **(G)** qRT-PCR analysis of expression levels of *PPARγ* mRNA in the liver tissues of p47phox^{-/-} and control mice exposed to FA or PM_{2.5} for 10 weeks. Fold changes of mRNA are shown by normalizing mRNA levels to that of the FA-exposed control animals. Each bar denotes the mean ± SEM (n=4 animals per group). For B, C, E, and G, * *P*<0.05.